Self-Assembly of ABA Amphiphilic Triblock Copolymers into Vesicles in Dilute Solution

Jintao Zhu,[†,‡] Ying Jiang,[§] Haojun Liang,*[,†,‡,§] and Wei Jiang*[,†,‡]

State Key Laboratory of Polymer Physics and Chemistry, Changchun Institute of Applied Chemistry, Chinese Academy of Sciences, Changchun 130022, People's Republic of China, Graduate School of the Chinese Academy of Sciences, People's Republic of China, and Department of Polymer Science and Engineering, University of Science and Technology of China, Hefei, Anhui 230026, People's Republic of China

Received: December 12, 2004; In Final Form: March 2, 2005

Self-assembly of an ABA amphiphilic triblock copolymer into vesicles in dilute solution was studied by successfully combining experimental methods and a real-space self-consistent field theory in three-dimensional space. It was found experimentally that vesicle size was sensitive to the initial copolymer concentration in the organic solvent. Also, the aggregate morphologies and vesicles sizes were found to be dependent on the annealing time. A number of complex vesicles, such as global, long-style, trigonal, and necklacelike vesicles, were obtained in our experiments. Moreover, the corresponding microstructures were produced in our simulations. The results show that various vesicles in dilute solution are formed solely on account of the inhomogeneous density distribution in the local region in nature. Our simulations confirm that the structural complexity coexisting behavior in the single-amphiphile systems is largely attributed to the metastability rather than the polydispersity of the triblock copolymer. These metastable states should strongly depend on the pathway of the system on the free energy landscapes, which is governed by the initial condition.

1. Introduction

It has been known for some years that highly asymmetric amphiphilic block copolymers can self-assemble in solution to form "crew-cut" aggregates of multiple morphologies.[1−3] These cornucopian morphologies include spheres, vesicles, rods, bicontinuous structures, lamellae, tubes, large compound vesicles, hexagonally packed hollow hoops, bowl-shaped and ring-shaped structures, and several others.[4−7] In such crew-cut aggregates, the relatively long blocks form the core, while the short ones form the corona.[2,3] Among the various morphologies, the closed bilayer membranes, vesicles, and other hollow spheres (including liposomes) are of special interest because of their scientific interest and potential applications.[8] The resemblance of synthetic vesicles to biological membranes makes them an attractive model for cells and organelles,[9,10] and their ability to offer both hydrophobic and hydrophilic domains suitable for incorporation opens the door for their application as microreactors,[11] environmental toxin sequesters, and drug delivery vehicles.[12−14] As polymers have higher stability and lower mobility than small-molecule amphiphiles, increasing interest is given to the study of polymeric vesicles.[15]

Up to now, polymeric vesicles have been prepared from a variety of materials, including amphiphilic coil−coil-type diblock copolymers[16−18] and peptide-based coil−rod diblock copolymers.[19,20] Only a few publications describe vesicle formation from asymmetric ABC [4,21,22] and symmetric ABA [23−25] triblock copolymers; for example, vesicles from the ABC triblock polystyrene-*b*-poly(methyl methacrylate)-*b*-poly(acrylic acid) (PS_{180}-*b*-$PMMA_{67}$-*b*-PAA_{37}) were prepared in a dioxane/H_2O mixture by Yu et al.[22] Vesicles from a poly(ethylene oxide)-*b*-poly(propylene oxide)-*b*-poly(ethylene oxide) (PEO-*b*-PPO-*b*-PEO) triblock copolymer have been studied by Schillén's group in dilute aqueous solution.[23] Recently, it has been reported that vesicles formed from poly(acrylic acid)-*b*-polystyrene-*b*-poly(4-vinyl pyridine)(PAA-*b*-PS-*b*-P4VP) prepared at pH* 1 contain P4VP chains on the outside and PAA chains on the inside, while those prepared from the same triblock at pH* 14 contain PAA outside and P4VP inside.[26]

The kinetics and mechanisms of various morphological transitions are theoretically important in understanding the changes that various aggregates can undergo.[27] The understanding of the mechanism for various aggregate morphologies formation is also of significance for many biological systems because some parts of living cells resemble the morphologies observed in block copolymer systems.[27−30] A mechanistic study of copolymer systems may thus shed some light on the structural changes in biological cells.[29,30] Many attempts have been made to study the vesicle formation mechanism in experiment[31−33] and theory.[32,34−40] Some possible pathways for the dynamic process of vesicle formation have been proposed, such as bending of a membrane, aggregation and rearrangement of small micelles, and fusion of small vesicles among others. However, the mechanism for the formation of these complex microstructures was not very clear until now.

Computer simulation and theoretical methods are useful tools in the study of the dynamic process and mechanism for the formation of those complex morphologies in situ. Various theoretical approaches, such as coarse-grained surface models,[32,34] Brownian dynamic simulations,[36,37] Monte Carlo simulations,[38,39] and dissipative particle dynamics (DPD), have been used to investigate the formation of vesicles and the dynamic process of self-assembly of amphiphilic molecules.[40] These methods focused on the self-assembly process of amphiphilic

* Authors to whom correspondenc should be addressed. E-mail: wjiang@ciac.jl.cn; hjliang@ustc.edu.cn.

[†] Changchun Institute of Applied Chemistry, Chinese Academy of Sciences.

[‡] Graduate School of the Chinese Academy of Sciences.

[§] Department of Polymer Science and Engineering, University of Science and Technology of China.

10.1021/jp044344d CCC: $30.25
Published on Web 04/02/2005

copolymers in a small sample space (only one or two vesicles are formed at terminal equilibrium). So it is unknown whether the same equilibrium can be obtained for a larger system. The longer computational time cost using a larger sample is beyond tolerance.

In addition, a type of self-consistent field theory (SCFT) has been successful in helping to explain the complex mesophases experimentally observed in block copolymers. SCFT, a mesoscopic simulation technique originated by Edwards in the 1960s, was adapted by Helfand and others to treat the self-assembly of block copolymers.[41−47] And this method has been widely applied to study the performance of block copolymers in solution.[46,47] In addition, another real-space self-consistent field, namely, dynamic density-functional theory (DDFT), was also used to understand the behaviors of block copolymers in solution and to capture the micelle shape and the mechanism of the resulting micelle formation.[48,49] However, in general, SCFT focuses on concentrated solutions (polymer concentration > 30%). At the same time, as a result of lower computational efficiency (for DDFT) and special requirements (the conventional SCFT is unsuitable for the discovery of previously unknown mesophases),[50] it is difficult to study the self-assembly of the block copolymers in dilute solution. Previously, Liang et al.[51] had successfully used a real-space SCFT approach as developed by Fredickson's group [50−53] to study the formation of mesophases of amphiphilic diblock copolymer in dilute solution in two-dimensional (2D) space. However, the terminal equilibrium, which is formed in 2D space, may be quite different with the one produced under real conditions. Therefore, it is expected to be able to predict the dynamics of the amphiphilic molecules and the self-assembly process into vesicles for the real space.

In this paper, experimental methods and the real-space self-consistent field theory in 3D space were combined to study the self-assembly of amphiphilic triblock copolymer into vesicles in dilute solution. The experimental results correlate well with the simulation predictions. A number of vesicles, such as global, long-style, trigonal, and necklacelike vesicles were obtained in experiment and simulation. Our calculations show that various vesicles in dilute solution are formed solely on account of the inhomogeneous density distribution in a local region in nature. In addition, our simulations confirmed that such structural complexity coexisting behavior in the single-amphiphile systems is largely attributed to the metastability rather than the polydispersity of the triblock copolymer.

2. Experimental Section

The copolymer used in this study is a triblock copolymer of $P4VP_{43}$-*b*-PS_{366}-*b*-$P4VP_{43}$, which was purchased from Polymer Source, Inc., Canada. (The numbers in the subscripts indicate the number of repeat units of the blocks. $M_n = 47\,000$ g/mol; PDI = 1.10.) To prepare the aggregates in aqueous solution, the triblock copolymer was dissolved in a dioxane/water mixture of varying water contents (25−30 wt %) by stirring for a few days. Dioxane is a good solvent for both types of blocks, while water is a good solvent only for the P4VP blocks but a precipitant for the PS blocks. (Although the P4VP block is not soluble in pure water, it is soluble in dioxane solutions containing up to 50 wt % water and is also soluble in water below pH 5.[54]) The initial copolymer concentration in organic solvent was 1−3 wt % for the samples. Then, a large amount of water was added to the resulting solution to quench the aggregate morphologies. At this water content range, the structures of the aggregates become kinetically locked over the experimental time scale. Subsequently, the resulting solution was placed in dialysis tubes and dialyzed against distilled water for a few days to remove all of the organic solvent from the solution. During the dialysis process, the pH of the distilled water was adjusted to 4 to keep the colloid solutions from precipitating.[54] The morphologies of the aggregates were stable during the dialysis process and after the dialysis. The length of time between dissolution of the copolymer into the solvent mixture and subsequent large amount of water addition is the annealing time.

The resulting aggregate morphologies were visualized by transmission electron microscopy (TEM). TEM was performed on a JEOL JEM-2000FX transmission electron microscope operated at an acceleration voltage of 160 kV. The dialyzed colloidal solutions were diluted by a factor of 10−20 to prepare the TEM samples. A drop of the very dilute solution was placed onto the TEM copper grid covered by a polymer support film precoated with carbon thin film. After 15 min, the excess solution was blotted away using a strip of filter paper. The samples were allowed to dry in atmosphere and at room temperature for 1 day before observation.

3. Theoretical Section

In this section, we outline the formulation of the self-consistent field theory (SCFT) for ABA amphiphilic triblock copolymer in dilute solution. Amphiphlic triblock copolymers with hydrophilic segments (A), hydrophobic segments (B), and solvent molecules (S) are dissolved in volume V. The volume fractions of segment A and B in the system are f_A and f_B, respectively. As a result, the volume fraction of copolymer and solvent in solution are $f_P = f_A + f_B$ and $f_S = 1 - f_P$, respectively. In real-space SCFT, one considers the statistics of a single copolymer chain in a set of effective chemical potential fields ω_I, where I represents block species A or B. These chemical potential fields, which replace the actual interactions between different components, are conjugated to the segment density fields, ϕ_I, of block species I. Similarly, solvent molecules are considered to be in an effective chemical potential field ω_S that conjugates to the solvent density field ϕ_S. Hence, the free energy function (in units of k_BT) of the system is given by

$$F = -f_S \ln(Q_S/V) - \frac{f_P}{N}\ln(Q_P/V) + \frac{1}{V}\int \mathrm{d}r[\chi_{AB}\phi_A\phi_B + \chi_{AS}\phi_A\phi_S + \chi_{BS}\phi_B\phi_S - \omega_A\phi_A - \omega_B\phi_B - \omega_S\phi_S - P(1 - \phi_A - \phi_B - \phi_S)] \quad (1)$$

where N is the length of the copolymer chain, χ_{ij} is the Flory−Huggins interaction parameter between species i and j, P is the Lagrange multiplier (as a pressure), $Q_S = \int \mathrm{d}r \exp(-\omega_S)$ is the partition function of the solvent in the effective chemical potential field ω_S, and $Q_P = \int \mathrm{d}r\, q(r,1)$ is the partition function of a single chain in the effective chemical potential fields of ω_A and ω_B. The end-segment distribution function $q(r,s)$ gives the probability that a section of a chain, of contour length s and containing a free chain end, has its "connected end" located at r. The parametrization is chosen such that the contour variable s increases continuously from 0 to 1, corresponding from one end of the chain to the other. With the use of a flexible Gaussian chain model to describe the single-chain statistics, the function $q(r,s)$ satisfies a modified diffusion equation.

$$\frac{\partial}{\partial s} q(r,s) = \nabla^2 q(r,s) - N\theta_i(s)\omega_i q(r,s) \quad (i = 1,2,3) \quad (2)$$

where $\theta_i(s)$ is equal to 1 if s belongs to block i and otherwise it is equal to 0. In eq 2, lengths are scaled by the (overall) radius of gyration of an unperturbed chain. The appropriate initial condition is $q(r,0) = 1$. Here, ω_I is ω_A when $0 < s < f_1$ and $f_1 + f_2 < s < 1$ and ω_B when $f_1 < s < f_1 + f_2$ (where f_i is the volume fraction of block i). Similarly, a second distribution function $q'(r,s)$ (containing another chain end) is also satisfied by eq 2 with the initial condition $q'(r,0) = 1$, but in this case ω_I is ω_A when $0 < s < f_3$ and $f_2 + f_3 < s < 1$ and ω_B when $f_3 < s < f_2 + f_3$. The density of each component is obtained by

$$\phi_{A(B)}(r) = \frac{1}{Q_P}\int_0^1 \mathrm{d}s\, q(r,s)q'(r,1-s)\theta_i(s)$$

$$\phi_S(r) = \frac{\exp(-\omega_S(r))}{Q_S} \tag{3}$$

From the equilibrium condition, i.e., minimization of the free energy to density and pressure, $\delta F/\delta\phi = \delta F/\delta P = 0$, this leads to another four equations.

$$\omega_A(r) = \chi_{AB}(\phi_B(r) - f_B) + \chi_{SA}(\phi_S(r) - f_S) + P(r)$$

$$\omega_B(r) = \chi_{AB}(\phi_A(r) - f_A) + \chi_{BS}(\phi_S(r) - f_S) + P(r)$$

$$\omega_S(r) = \chi_{SA}(\phi_A(r) - f_A) + \chi_{BS}(\phi_B(r) - f_B) + P(r)$$

$$\phi_A(r) + \phi_B(r) + \phi_S(r) = 1 \tag{4}$$

Here, constant shifts in the potential are introduced in the equations.

The method is to search for low free energy solutions of the equations within a planar square or box with a periodic boundary condition. The initial value of ω is constructed by $\omega_j(r) = \Sigma_{i\neq j}\chi_{ij}(\phi_i(r) - f_i)$, where f_i represents the average volume fraction of the copolymer segments and solvents and $\phi_i(r) - f_i$ satisfies the Gaussian distributions

$$\langle(\phi_i(r) - f_i)\rangle = 0$$

$$\langle(\phi_i(r) - f_i)(\phi_j(r') - f_j)\rangle = \beta f_i f_j \delta_{ij}\delta(r - r') \tag{5}$$

Here, β is defined as the density fluctuation at the initial temperature. The effective pressure field, $P = C_2C_3(\omega_A + \omega_B) + C_1C_3(\omega_B + \omega_S) + C_1C_2(\omega_A + \omega_S)/2(C_1C_2 + C_2C_3 + C_1C_3)$, on each grid is obtained through solving eq 4, where $C_1 = \chi_{SA} + \chi_{BS} - \chi_{AB}$, $C_2 = \chi_{SA} + \chi_{AB} - \chi_{BS}$, and $C_3 = \chi_{AB} + \chi_{BS} - \chi_{SA}$. The density field ϕ_I of species I, conjugated to the chemical potential field ω_I, can be evaluated based on eqs 2 and 3. The chemical potential field ω_I can be updated by using the equation $\omega_I^{new} = \omega_I^{old} + \Delta t(\delta F/\delta\phi_I)^*$ where $(\delta F/\delta F_I)^* = \Sigma_{M\neq I}\chi_{IM}(\phi_M(r) - f_M) + P(r) - \omega_I^{old}$ as the chemical potential force. In our simulation, the time step $\Delta t = 0.3$, and the above steps are iterated until the free energy converges to a local minimum, where the phase structure corresponds to a metastable state. This iteration scheme is a pseudodynamics process with a steepest descent on the energy landscape to the nearest metastable solution. It is possible to reach various metastable states depending on the initial conditions.

The numerical simulation was on the three-dimensional space with a $50 \times 50 \times 50$ cubic lattice with space $L = 16.666$ and grid size $\Delta x = 0.3333$ in the unit of R_g (unperturbed mean-square radius of gyration of a copolymer chain). The simulations for each sample are carried out until the phase patterns are stable and invariable with time and $\Delta F < 10^{-6}$. The simulation of the homogeneous block copolymer solution was reiterated from 10 to ~20 times from different initial random states and different random numbers to ensure that the phenomena are not accidental. In the present simulation, the length of chain N equals 68, the length fraction of the A block equals 0.147, which corresponds to our experimental value 0.190, and $f_P = 0.1$ to ensure that the system is in dilute solution. In particular, we consider ABA triblocks that are symmetric about their midpoint; i.e., the **A** blocks are fixed to be equal length (equal volume fractions $f_1 = f_3$).

4. Results and Discussion

Due to the higher composition of the hydrophobic PS blocks (volume fraction 80.3%), the triblock copolymer ($P4VP_{43}$-*b*-PS_{366}-*b*-$P4VP_{43}$) cannot be dissolved in water directly. However, the copolymer can be dissolved in a dioxane/water mixture of varying water content, followed by stirring (annealing) for a few days. The aggregate morphologies were formed during the annealing process. Then, the aggregates were isolated into water by dialyzing the resulting solutions against distilled water to remove all of the dioxane from the solution. At some point, however, as the dioxane was forced out of the PS core during the large amount of water addition and the subsequent dialysis, the equilibrium was frozen because of the glassy nature of the PS chains.[2] Figure 1 shows the TEM images of the aggregate morphologies formed from $P4VP_{43}$-*b*-PS_{366}-*b*-$P4VP_{43}$ in a dioxane/water mixture with 25 wt % water content after annealing for 3 days. From Figure 1, we can see that dominant aggregate morphology is the vesicle. The vesicular nature is shown from a higher transmission in the center of the aggregates than around their periphery, [22] coupled with the atomic force microscopy (AFM) height measurement, which shows the aggregates to be spherical (Supporting Information).

The stretching and structures of the triblock copolymer consisting of vesicles are different from the diblock copolymers and other types of block copolymers. A schematic representation of P4VP-*b*-PS-*b*-P4VP crew-cut vesiclular micelles in aqueous solution was given in Figure 2. In the vesicles, the insoluble blocks constitute the vesicle wall, while the chains of soluble blocks extend from the inner and outer surfaces into the solvent system (Figure 2). These aggregates involve the looping of the hydrophobic PS middle block into the core of the aggregates and the tailing of two hydrophilic P4VP end blocks to form the corona of the aggregates.

The overall sizes of the vesicles were found to be sensitive to the initial copolymer concentration in dioxane. For example, the vesicles, formed from 1 wt % of the copolymer in dioxane, were relatively uniform and small (average diameter of the vesicles was 203 nm). For the vesicles formed from 3 wt % of this copolymer in dioxane, the sizes are very polydispersed and large (average diameter 472 nm). Figure 1b partially displays a giant vesicle with a diameter of at least several micrometers, coexisting with complex small-sized (<300 nm) vesicles. The vesicles' diameter distribution with different initial copolymer concentrations is given in Figure 3. When the initial concentration of the copolymer was increased to 3 wt %, the vesicle sizes were polydispersed, with the outside radii (R_{out}) ranging from 90 to 2470 nm. Some vesicles with micrometer-sized diameters (maximal diameter found in experiment was 2.4 μm) were frequently found in experiment. However, the PS wall thickness of the vesicles was very uniform and independent of the overall sizes of the vesicles. From these TEM images, we estimated a fairly uniform bilayer thickness of 23 ± 2 nm by tracing the density profile as a function of distance across the core domain.

(a)

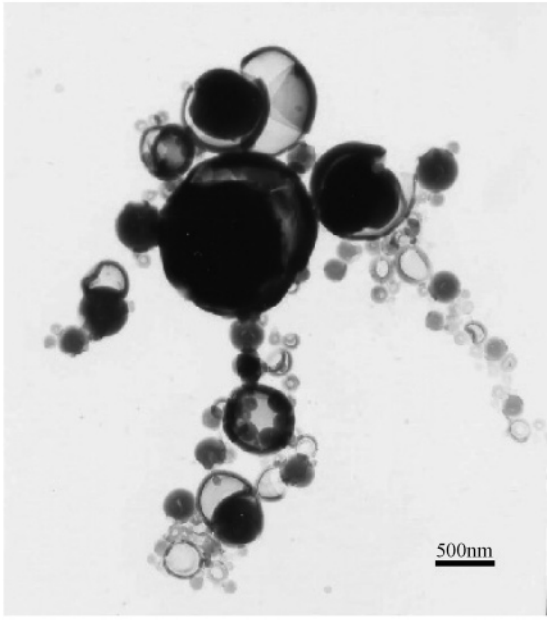

(b)

Figure 1. TEM images of vesicles formed from $P4VP_{43}$-*b*-PS_{366}-*b*-$P4VP_{43}$ in a dioxane/water mixture with 25 wt % water content after annealing for 3 days. The initial copolymer concentrations in dioxane were (a) 1 wt % and (b) 3 wt %.

It was found that the aggregate morphologies depended on the annealing time. Experimentally, prolonging the annealing time was favorable for the vesicle formation. A similar result has been deduced by Yu and Eisenberg for AB diblock copolymers.[30] It has been suggested that, in general, longer annealing times facilitate the formation of bilayer morphologies. However, when the annealing time was increased, the vesicle sizes would become more polydispersed. The giant vesicles may result from the fusion of small vesicles.

Moreover, from the TEM images displayed in Figure 1, we can find various vesicles. In addition to a normal spherical topology, these triblock copolymer vesicles exhibit a variety of shapes under the present preparation conditions. Figure 4 shows

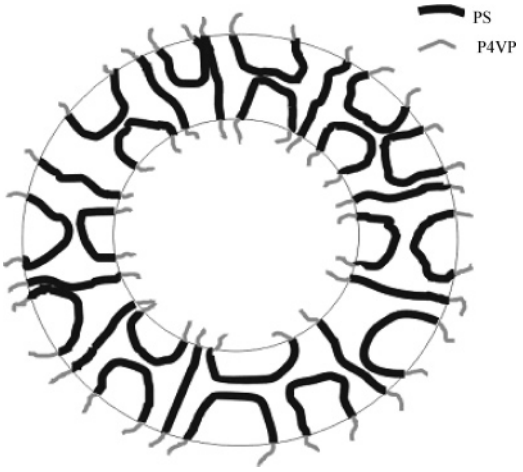

Figure 2. Schematic representation of P4VP-*b*-PS-*b*-P4VP crew-cut vesiclular micelles in aqueous solution.

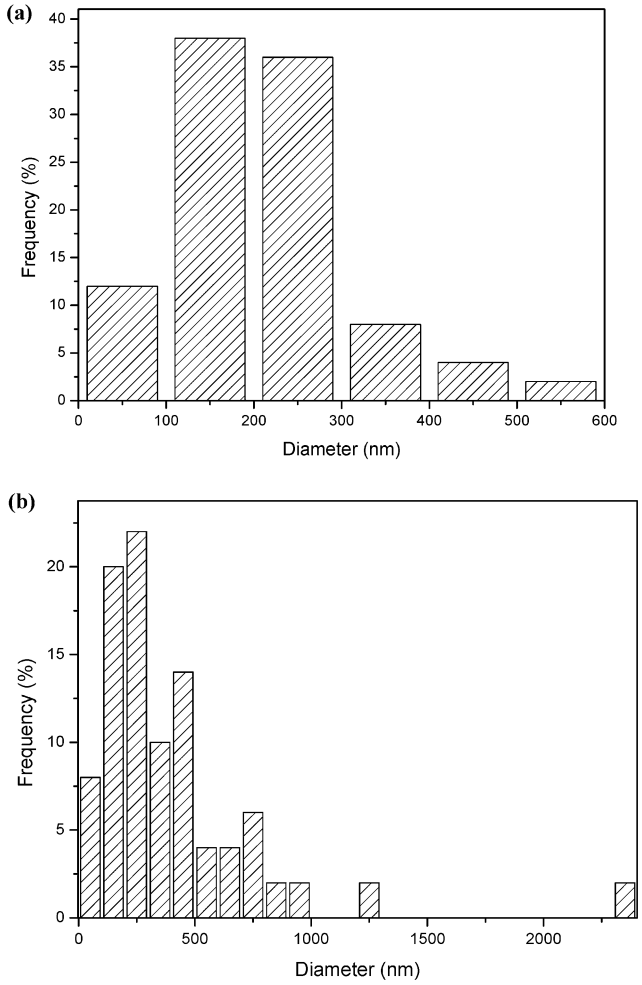

Figure 3. Diameter size distribution of the vesicles formed from the triblock copolymer (in a dioxane/water mixture with 25 wt % water content, corresponding to Figure 1) with different initial copolymer concentrations in dioxane after annealing for 3 days: (a) 1 wt % and (b) 3 wt %. The size distribution was obtained from several micrographs of the same morphology in each system by measuring the diameters of 200 vesicles.

part of the typical vesicles with different shapes, such as long-style, trigonal, global, and necklacelike vesicles (or biconcave shape, like that typical of red blood cells), from both experiment and simulation. Because periodic boundary conditions are used in our simulation, the end of the necklacelike vesicle in the

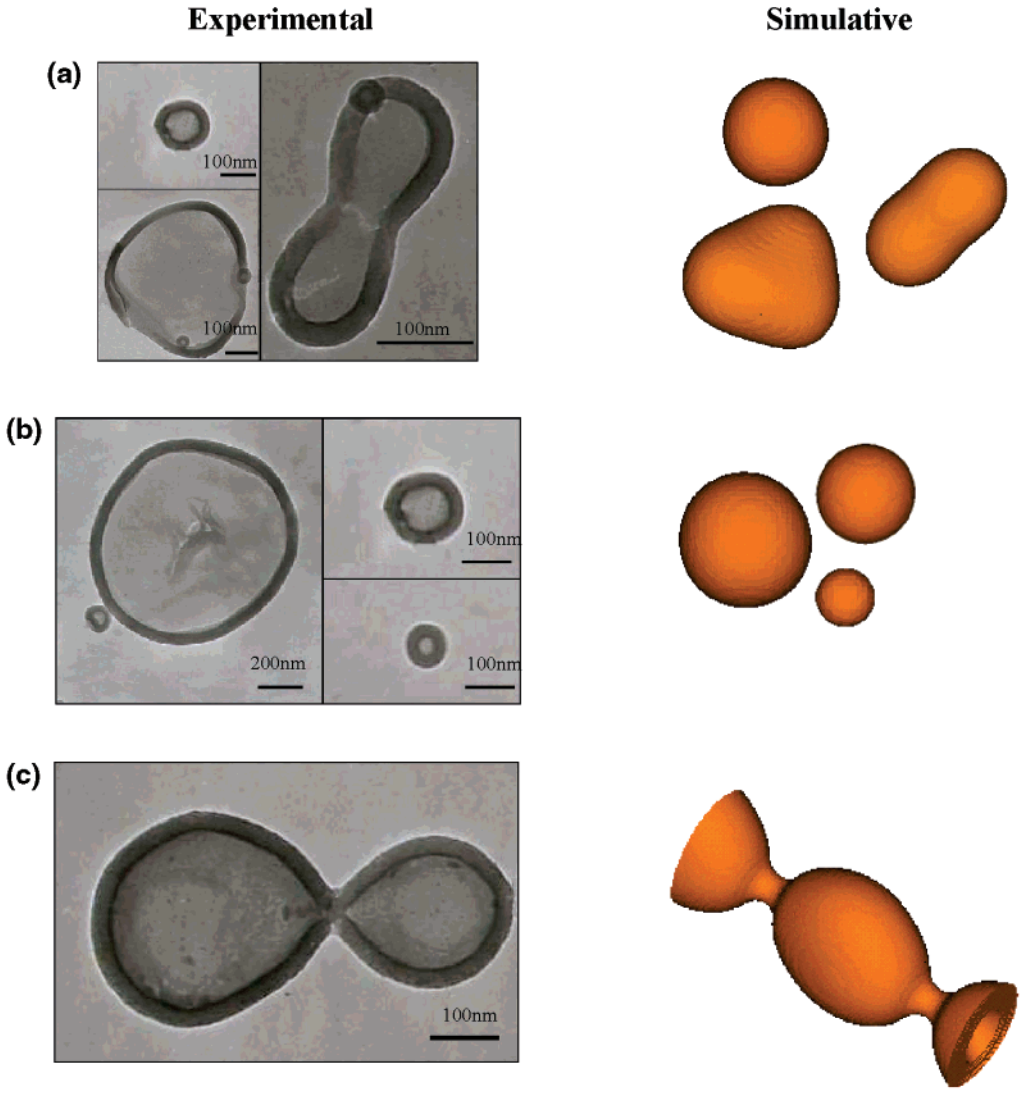

Figure 4. Microphases of the amphiphilic triblock copolymer in dilute solution from different values of the initial density fluctuation β and relative free energy F, with $\chi_{AB}N = 18.7$, $\chi_{BS}N = 22.1$, $\chi_{AS}N = -8.5$: (a) $\beta = 1.0 \times 10^{-2}$, $F = 0.7262$; (b) $\beta = 0.16$, $F = 0.7469$. For the purpose of comparison, corresponding TEM micrographs are also given in this figure. The microstructures were formed from 1 to 3 wt % $P4VP_{43}$-*b*-PS_{366}-*b*-$P4VP_{43}$ in a dioxane/water mixture with 25 wt % water content after annealing for 1−3 days.

simulation image (Figure 4c) has not been closed. It was seen that the simulation results correlate well with those of the experiment.

The main focus in the simulation is on the investigation of amphiphilic triblock copolymers ABA corresponding to real copolymers P4VP-*b*-PS-*b*-P4VP to assemble into vesicles in dilute solution. Considering the hydrophilic P4VP (A) block and the hydrophobic PS (B) block in our system, we provide the microstructural patterns (Figure 4) of triblock copolymers with interaction parameters $\chi_{AB}N = 18.7$, $\chi_{AS}N = -8.5$, and $\chi_{BS}N = 22.1$. Note that due to the limitation of the size of our simulation space the size of vesicles in our simulation cannot quantitatively correspond to the real sizes of vesicles in experiment. To clearly illustrate the microstructures in Figure 4, we present the cross sections of the different microphases in Figure 5. As noticed in Figure 5, solvent completely dominates the center of the irregular core while the hydrophobic segments distribute around the central solvent, forming the shell. Obviously, all three different microphases (Figure 5) are vesicles. In addition, we also notice that the hydrophilic blocks A in Figure 5 prefer to aggregate at the inner surfaces of vesicles, though the chemical nature of the inner and outer environments of the vesicles is the same. It can be explained as follows: Due to the limitations in the size of the vesicles, the hydrophilic blocks A inside the vesicles are not able to stretch completely in comparison with the ones outside the vesicles. So the distribution of the hydrophilic A blocks is not symmetric about the core of the hydrophobic B blocks. Similar to our previous simulation for the amphiphilic diblock in the dilute solution,[51] our results here also reveal that the microstructures of these vesicles depend significantly on a parameter referred to as the initial density fluctuation amplitude β, indicated by eq 5. This point is important for us to understand the aggregation features of block copolymers in dilute solution, as shown below.

A remarkable aspect disclosed by our TEM imaging of the polymeric aggregates is the coexistence of disparate morphologies for a single copolymer. Figure 6 shows the TEM image of the aggregate morphologies formed from the 1 wt % triblock copolymer in a dioxane/water mixture (water content 25 wt %) after being annealed for 1 day. From the TEM image (as can also be seen from Figure 1), we can clearly see the various coexisting morphologies. There are vesicles with different sizes and shapes, lamellar, spheres, etc. in Figure 6. These coexisting morphology phenomena are generally found in other polymeric aggregate systems.[3,55,56] It has been proposed that the polydispersity inherent in macromolecular samples is one factor that

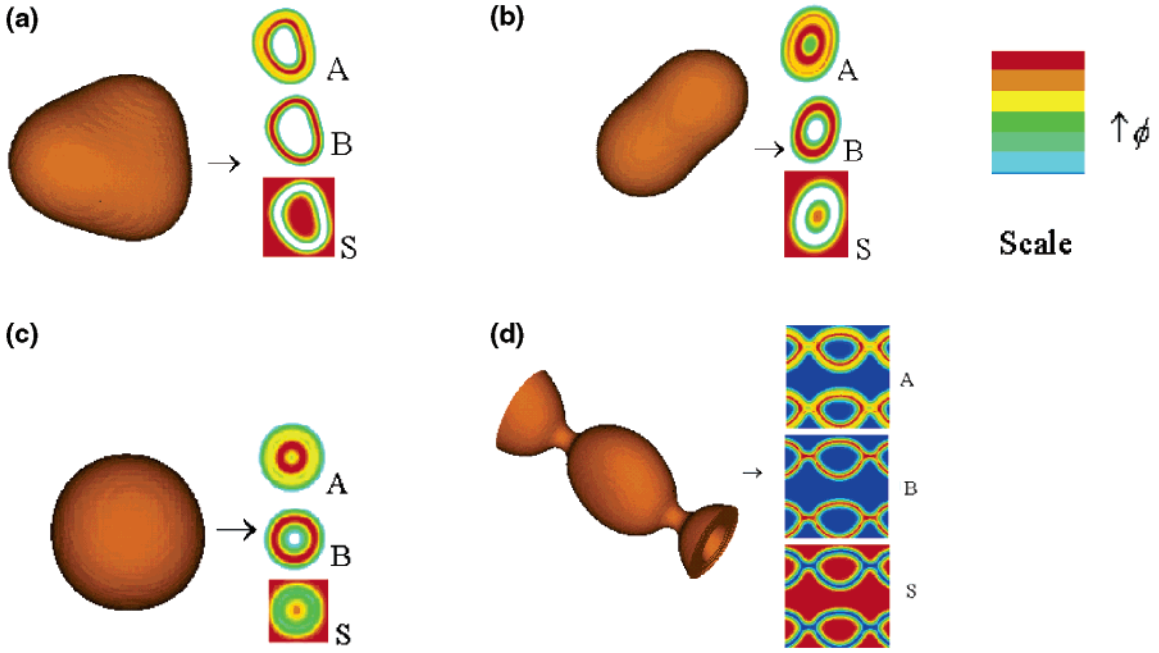

Figure 5. Four different types of vesicles formed from the self-assembly of the triblock copolymer and the corresponding cross-section pictures of different components (A, block A; B, block B; S, solvent.) are shown. In these cross-section pictures, the values, which are less than 25% of the corresponding maximum density in the region, are ignored for clarity. The scale is identical for all of the cross-section pictures. (a) The cross section approximately cuts the trigonal vesicle into two halves. (b) The cross section is perpendicular to the axial line of the long-style vesicle. (c) The cross section is along the diameter of the global vesicle. **(**d) The cross section is parallel to axial line of the necklacelike vesicle.

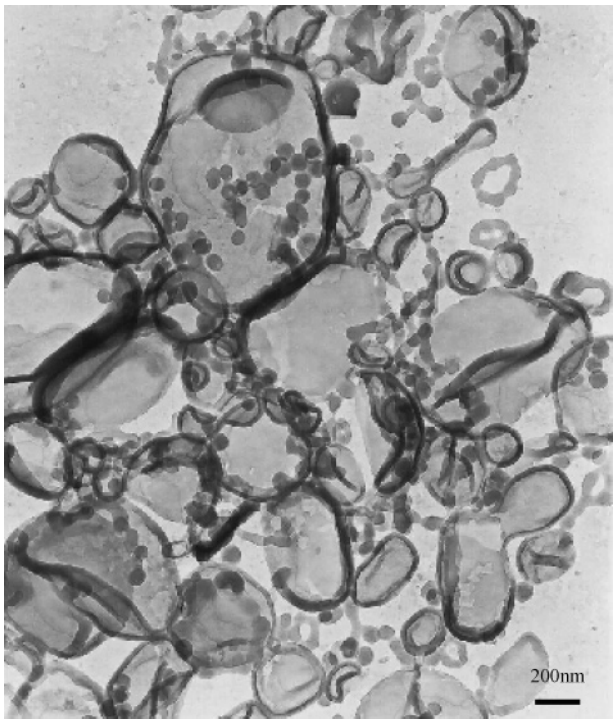

Figure 6. TEM image of coexisting aggregate morphologies formed form the 1 wt % $P4VP_{43}$-*b*-PS_{366}-*b*-$P4VP_{43}$ in a dioxane/water mixture with 25 wt % water content after being annealed for 1 day

at least partially contributes to the coexistence behavior.[55] The crucial insight is that slow kinetics associated with the high molecular masses may greatly hinder structural evolution toward global equilibrium after the genesis of the structures.[56] It is noteworthy that the individual objects formed in water by the block copolymer are practically isolated and the coexistence most likely represents nonequilibrium states, i.e., the structure initially formed upon dissolution will likely be locked in. Fortunately, we can get a deep understanding for the morphology coexistence behavior from simulation. On the basis of our simulation result, as stated above, the final structures depend on the initial density fluctuation amplitude β. According to this conclusion, we can conceive that for a macroscale homogeneous solution it will show some inhomogeneous characteristics on the microscale. For example, the density of polymer chains, i.e., the number of polymer chain per unit volume, in solution should be inhomogeneous on the microscale, which should constantly fluctuate with certain density amplitudes due to Brownian motion. Once phase separation occurs, those preaggregated chains due to density fluctuation should act as a "nucleus", from which phase growth starts. Thus, the fluctuation with smaller and larger amplitudes will lead to some very different morphologies, and the initial density should significantly affect the final structures. In applications of real-space SCFT to concentrated solutions and melts, the dependence of the final microstructures on β is not found because the initial density fluctuation amplitude is so small compared to the original density that its influence on the final patterns can be ignored. However, in the cases of dilute solution, the initial density fluctuation amplitude is comparable to its original density, and the influence of the initial density fluctuations can no longer be ignored. In fact, the free energies in Figures 4a and 4b in our simulation are $F = 0.7262$ and 0.7469, respectively. Obviously, in each case, the system does not correspond to the lowest free energy but has been trapped in different high free energy states, i.e., in a set of metastable states. This explains why different micromorphologies for a given block copolymer in the dilute solution can be produced through different manipulation procedures in experiments and the coexisting morphology phenomena. Thus, such structural complexity coexistence behavior in the single-amphiphile systems is largely attributed to the metastability rather than the polydispersity of the triblock copolymer. These metastable states should strongly depend on the pathway of the system on the free energy landscape, which is governed by the initial condition.

5. Conclusions

Aggregate morphologies of ABA amphiphilic triblock copolymers in dilute solution were studied by successfully combining the experimental method and the real-space self-consistent field theory. It was found in experiment that vesicle sizes were sensitive to the initial copolymer concentration in organic solvent. Also, the aggregate morphologies and vesicle sizes were found to be dependent on the annealing time. A number of vesicles, such as global, long-style, trigonal, and necklacelike vesicles were obtained in the experiment. Moreover, nearly the same microstructures as the experimental ones can be formed depending on the different initial density fluctuation amplitude β. The results show that various vesicles in dilute solution are formed solely on account of the inhomogeneous density distribution in the local region in nature. Our simulations confirm that structural complexity coexistence behavior in single-amphiphile systems is largely attributable to the metastability rather than the polydispersity of the triblock copolymer. These metastable states should strongly depend on the pathway of the system on the free energy landscape, which is governed by the initial condition.

Acknowledgment. We are grateful for the financial support of the General Program (203074050) and the Major Program (20490220) of the National Natural Science Foundation of China (NSFC), the Chinese Academy of Sciences (KJCX2-SW-H07), the 973 Program of MOST (2003CB61560), and the Fund for the Excellent Youth of Jilin Province, China.

Supporting Information Available: AFM images and their cross sections of the vesicles corresponding to Figure 1. This material is available free of charge via the Internet at http://pubs.acs.org.

References and Notes

(1) *Structure and Dynamics of Membranes*; Lipowsky, R.; Sackmann, E., Eds.; Elsevier Science: Amsterdam, 1995; Vol. 1A.
(2) Zhang, L. F.; Eisenberg, A. *Science* **1995**, *268*, 1728.
(3) Cameron, N. S.; Corbierre, M. K.; Eisenberg, A. *Can. J. Chem.* **1999**, *77*, 1311.
(4) Ding. J.; Liu, G. *Macromolecules* **1997**, *30*, 655.
(5) Discher, B. M.; Won, Y. Y.; Ege, D. S.; Lee, J. C. M.; Bates, F. S.; Discher, D. E.; Hammer, D. A. *Science* **1999**, *284*, 1143.
(6) Krämer, E.; Förster, S.; Göltner, C.; Antonietti, M. *Langmuir* **1998**, *14*, 2027.
(7) Zhu, J. T.; Liao, Y. G.; Jiang, W. *Langmuir* **2004**, *20*, 3809.
(8) Choucair, A.; Lavigueur, C.; Eisenberg, A. *Langmuir* **2004**, *20*, 3894.
(9) Nardin, C.; Windmer, J.; Winterhalter, M.; Meier, W. *Eur. Phys. J. E* **2001**, *4*, 403.
(10) Hammer, D.; Disher, D. E. *Annu. Rev. Mater. Res.* **2001**, *31*, 387.
(11) Vriezema, D. M.; Hoogboom, J.; Velonia, K.; Takazawa, K.; Christanen, P. C. M.; Maan, J. C.; Rowan, A. E.; Nolte, R. J. M. *Angew. Chem., Int. Ed.* **2003**, *42*, 772.
(12) Dufes, C.; Schatzlein, A. G.; Tetley, L.; Gray, A. I.; Watson, D. G.; Olivier, J.-C.; Couet, W.; Uchegbu. I. F. *Pharm. Res.* **2000**, *17*, 1250.
(13) Lee, J. C. M.; Bermudez, H.; Discher, B. M.; Scheehan, M. A.; Won, Y. Y.; Bates, F. S.; Discher, D. E. *Biotechnol. Bioeng.* **2001**, *73*, 135.
(14) Photos, P. J.; Bacakova, L.; Discher, B.; Bates, F. S.; Discher, D. E.; *J. Controlled Release* **2003**, *90*, 323.
(15) Shen, H.; Eisenberg, A. *Angew. Chem., Int. Ed.* **2000**, *39*, 3310.
(16) van Hest, J. C. M.; Delnoye, D. A. P.; Baars, M. W. P. L.; van Genderen, M. H. P.; Meijer, E. W. *Science* **1995**, *268*, 1592.
(17) Maskos, M.; Harris, J. R. *Macromol. Rapid. Commun.* **2001**, *22*, 271.
(18) Harris, J. K.; Rose, G. D.; Bruening, M. L. *Langmuir* **2002**, *18*, 5337.
(19) Cornlissen, J. J. L. M.; Fischer, M.; Sommerdijk, N. A. J. M.; Nolte, R. J. M. *Science* **1998**, *280*, 1427.
(20) Kukula, H.; Schlaad, H.; Antonietti, M.; Förster, S. *J. Am. Chem. Soc.* **2002**, *124*, 1658.
(21) Stoenescu, R.; Meier, M. *Chem Commun.* **2002**, 3016.
(22) Yu, G.; Eisenberg, A. *Macromolecules* **1998**, *31*, 5546.
(23) Schillén, K.; Bryskhe, K.; Mel'nikova, Y. S. *Macromolecules* **1999**, *32*, 6885.
(24) Nardin, C.; Hirt, T.; Leukel, J.; Meier, W. *Langmuir* **2000**, *16*, 1035.
(25) Chen, X. L.; Jenekhe, S. A. *Macromolecules* **2000**, *33*, 4610.
(26) Liu F.; Eisenberg, A. *J. Am. Chem. Soc.* **2003**, *125*, 15059.
(27) Chen, L.; Shen, H.; Eisenberg, A. *J. Phys. Chem. B.***1999**, *103*, 9488.
(28) Kakorin, S.; Stoylov, S. P.; Neumann, E. *Biophys. Chem.* **1996**, *58*, 1.
(29) Luo, L.; Eisenberg, A. *Langmuir* **2001**, *17*, 6804.
(30) Yu. K.; Eisenberg, A. *Macromolecules* **1998**, *31*, 3509.
(31) Farquhar, K. D.; Misran, M.; Robinson, B. H.; Steytler, D. C.; Morini, P.; Garrett, P. R.; Holzwarth, J. F. *J. Phys.: Condens. Matter* **1996**, *8*, 9397.
(32) Lipowsky, R. *Nature* **1991**, *349*, 475.
(33) Bernardes, T. *Langmuir* **1996**, *12*, 5763.
(34) Jülicher. F.; Lipowsky, R. *Phys. Rev. Lett.***1993**, *70*, 2964.
(35) Umeda, T.; Nakajima, H.; Hotani, H. *J. Phys. Soc. Jpn.* **1998**, *67*, 682.
(36) Noguchi, H.; Takasu, M. *Phys. Rev. E* **2001**, *64*, 041913.
(37) Noguchi, H.; Takasu, M. *J. Chem. Phys.* **2001**, *115*, 9547.
(38) Bernardes, A. T. *J. Phys. II* **1996**, *6*, 169.
(39) Bernardes, A. T. *Langmuir* **1996**, *12*, 5763.
(40) Yamamoto, S.; Maruyama, Y.; Hyodo, S.-A. *J. Chem. Phys.* **2002**, *116*, 5842.
(41) Edwards, S. F. *Proc. Phys. Soc.* **1965**, *85*, 613.
(42) Helfand, E. *J. Chem. Phys.* **1975**, *62*, 999.
(43) Matsen, M. W.; Schick, M. *Phys. Rev. Lett.* **1994**, *72*, 2660.
(44) Noolandi, J.; Shi, A.-C.; Linse, P. *Macromolecules* **1996**, *29*, 5907.
(45) Bohbot-Raviv, Y.; Wang, Z. G. *Phys. Rev. Lett.* **2000**, *85*, 3428.
(46) Riess, G. *Prog. Polym. Sci.* **2003**, *28*, 1107.
(47) Linse, P. Modelling of the Self-Assembly of Block Copolymers in Solution. In *Amphiphilic Block Copolymers: Self-Assembly and Applications*; Alexandridis, P., Lindman, B., Eds.; Elsvier: Amsterdam, 2000; pp 13−40.
(48) van Vlimmeren, B. A. C.; Maurits, N. M.; Zvelindovsky, A. V.; Sevink, G. J. A.; Fraaije, J. G. E. M. *Macromolecules* **1999**, *32*, 646.
(49) Guo, S. L.; Hou, T. J.; Xu, X. J. *J. Phys. Chem. B* **2002**, *106*, 11397.
(50) Fredrickson, G. H.; Ganesan, V.; Drolet, F. *Macromolecules* **2002**, *35*, 16.
(51) He, X. H.; Liang, H. J.; Huang, L.; Pan, C. Y. *J. Phys. Chem. B* **2004**, *108*, 1731.
(52) Drolet, F.; Fredrickson, G. H. *Macromolecules* **2001**, *34*, 5317.
(53) Drolet, F.; Fredrickson, G. H. *Phys. Rev. Lett.* **1999**, *83*, 4317.
(54) Shen, H. W.; Zhang, L. F.; Eisenberg, A. *J. Am. Chem. Soc.* **1999**, *121*, 2728.
(55) Zhang, L. F.; Eisenberg, A. *Polym. Adv. Technol.* **1998**, *9*, 677.
(56) Won, Y. Y.; Brannan, A. K.; Davis, H. T.; Bates, F. S. *J. Phys. Chem. B* **2002**, *106*, 3354.